The Journal of Engineering Geology, Vol.4, No.1, April., 1994., pp.1-11

Mechanical Behavior of Cracked Rocks with Biotite Contents
크랙을 갖는 암반에서의 역학적 거동

정교철(Jeong, Gyo Cheol)	한국자원연구소
清木隆文(Seiki, Takafumi)	Nagoya University
市川康明(Ichikawa, Yasuaki)	Nagoya University
김원영(Kim, Won Young)	한국자원연구소
김영기(Kim, Young Ki)	경북대학교

요약/Abstract

In general there are many cracks in rocks. In this study, we are concerned with the mechanical effect on cracks on the behavior of rocks. For this purpose, we used specimens made of mortar having one crack set which has a constant length and same direction. Orientation of this set was varied with respect to the loading axis. We did a number of uniaxial experiments and observed propagation of the crack set to understand the effect set of the geometry of the crack set and its location on the mechanical behavior of the rocks with distributed crack sets. Finally, we analysed our experiments by FEM elastic analyses and Homogenization theory.

일반적으로 암반에는 크고작은 크랙들이 많이 분포하고있다. 이들 크랙들은 그암반의 역학적 거동에 크게 영향을 미친다는 것은 잘 알려져 있는 사실이다.

본 연구에서는 암반의 역학적 거동에 미치는 크랙의 기하학적 영향과 그 크랙끝에 집중하는 응력의 크기가 해석되었다. 이를위해, 모델실험으로서 여러 크랙셑을 가지는 모르타르 공시체를 제작하였으며, 이들 공시체를 가지고 일축압축실험을 실시하였다. 실험도중 크랙의 발생과 진전을 직접 그리고 연속적으로 관찰하기위해 비데오시스템이 설치되었다. 또한 응력-변형 곡선 역시 퍼스날 컴퓨터에의해 기록되었다.

이들의 수치해석은 유한요소법과 균질화 이론에 의해 해석되었다. 이들 해석치는 암반중에 분포하는 크랙의 진전 메카니즘과 역학성을 정량적으로 잘 설명해준다.

INTRODUCTION

Rock is a natural material with some pre−existing cracks and its mechanical properties are strongly dependent on cracks and cavities occurring during loading. The problem of the description of inelastic behavior of rock is essential for the solution of numerous boundary−value problems in engineering geology and civil engineering (e.g., underground space development and radioactive waste disposal) (Jeong, 1994).

The development of underground space has been becoming an attractive option, particularly in / around the metropolitan cities such as Tokyo, Osaka in Japan (Seiki et al., 1993). Therefore, the ground conditions are of great interest for the design and construction of underground structures. As underground structures are of large scale, the assessment of the stability of the structures is of paramount importance.

Failure of biotite−bearing rocks during complex loading could result from microstructures of the biotites and related cracking (Shea et al., 1993 ; Jeong, 1994). That is, cleavage planes in biotite are generally those planes with the lowest bond density or strength, and lowest surface energy (Brace and Walsh, 1962). Thus strain energy stored in the grain as a result of applied stresses will tend to be relieved on those planes.

Our petrographic observations also show that low−angle cracks within quartz and feldspar grains of granite samples deformed in compression are commonly associated with the ends of biotite grains with inclined cleavage cracks (Fig. 1), which reveals in the same experimental results of Gottschalk (1990) and Wong et al. (1985).

In this study we are concerned with the mechanical effects of cracks on the behavior of rocks. For this purpose, we used specimens made of mortar having one crack set which has a constant length and same direction. And orientation of this set was varied with respect to the loading axis. We did a number of uniaxial experiments and observed propagation of the crack set to understand the effect of the geometry of the crack set and its location on the mechanical behavior of the masses with distributed crack sets.

Finally, we analyzed our experiments by FEM and Homogenization theory.

EXPERIMENTS

Specimen Preparation

The specimen size of rectangular prisms is 320mm×150mm×45mm and all specimens were made of mortar by using an early age hardening portland cement and standard sand. These materials are mixed by the following weight ratio (early age hardening portland cement : sand : water=1 : 0.85 : 0.42). To mix mortar material we used electrical mixer. And then we casted mortar into each mold. We used electrical viblator and plastic hammer to release air from mortar and compact it.

For every batch we prepared three recta-

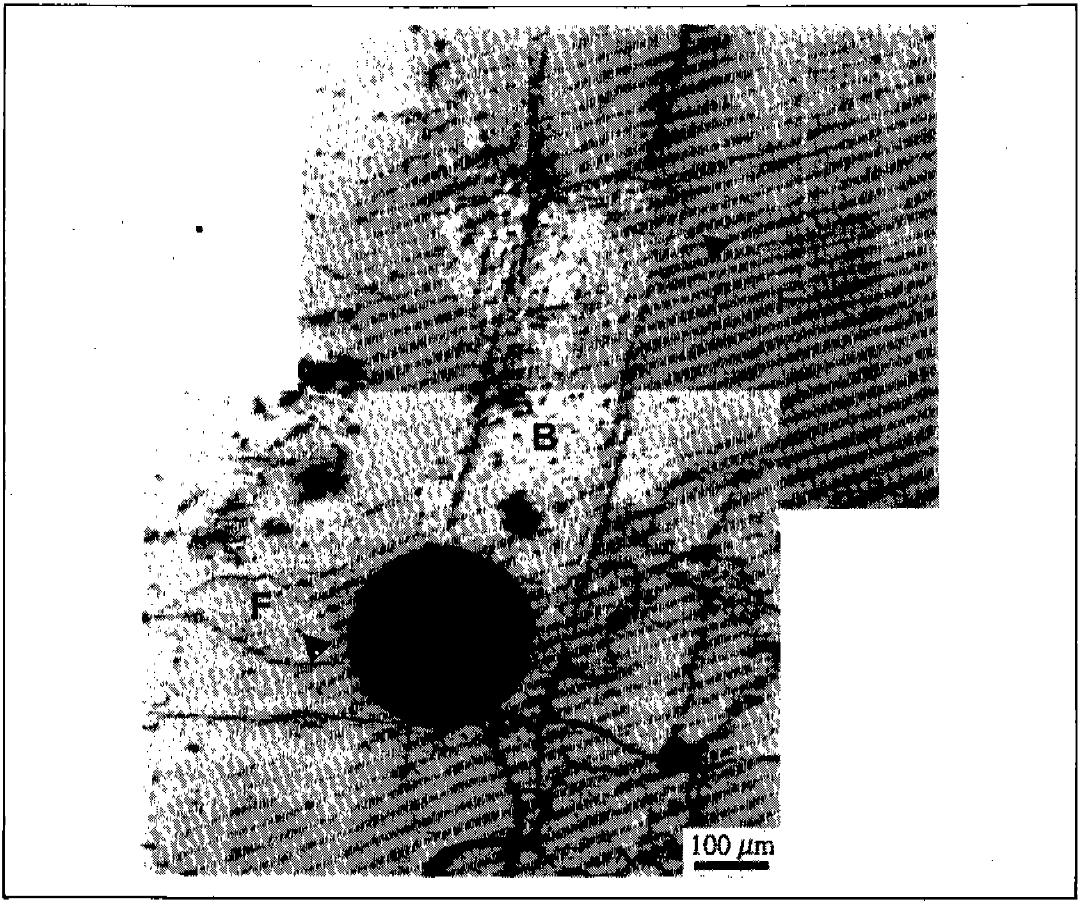

Fig.1 Geometrical relationships between biotite(B) with cracks and propagation of stress—induced cracks in feldspar (F). Axial stress direction is horizontal.

ngular prism specimens. Two of three specimens have 18 slits (Fig. 2) as initial cracks. We varied slit angle from 15° to 75° by an increment of 15°. At first to make slits in specimens we laid an ulethane sheet which is 5mm thick to maintain the opening state of initial crack at the bottom side of it. And then after modeling we inserted 18 steel strips, which are 26mm wide, 0.5mm thick and 60mm deep and were fixed on an acrylic plate by screws. Steel strips were coated grease to pull out them easily. Finally after 4 hours later from casting they were pulled out.

In another series we made specimens, which have a less number of slits, in order to observe crack propagation easily. These specimens had two or three rows of slits with an inclination with 0°.

After one day three specimens were removed from mold, and then cured for 6 days in

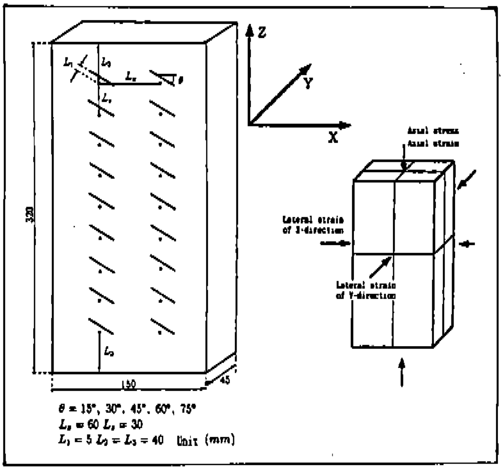

Fig.2 Mortar specimen ; measuring elements and absolute axis on the specimen.

water. After curing the specimens were tested. The curing time was determined from the stabilization of specimens in strength and the efficiency of experimental work. The curing was done in a room whose temperature was always maintained at 20℃.

Experimental Procedure

Uniaxial compression test was carried out by high stiffness compression testing machine which has 100 ton loading capacity and stiffness of 3.04×10^2MN/m. The strain rate was 0.025 %/min. In experiments, axial stress, axial strain and lateral strain were measured. The analog data of load and displacements were measured at every 3 second and transformed into digital data. And then the digital data were stored on personal computer and the stress and strain response on real time were displayed on the monitor.

In order to observe crack propagation, the specimens were photographed and video-taped by a VTR system. For this purpose we used 8 mm video camera which could take 30 pictures per second and set up the shutter speed at 1/10000 sec for one picture. The video pictures were printed as a static picture by a using video printer. The photographs were used to obtain the value of crack propagation in relation to the stess and strain response.

We painted plaster to observe cracks more easily on the XZ-surface of a specimen. When the specimen is cracked, the plaster layer on the surface is also cracked and its white color can emphasis the crack as a black trace. Fig. 3 shows cracked mortar specimen.

EXPERIMENTAL RESULTS

Mechanical Properties

We determined the parameters such as peak strength, elastic modulus and Poisson's ratio from the experimental data, and normalized the damage parameters of the specimens having slits by the parameters of intact specimen in each batch. Fig. 4 shows the typical stress-strain relations for the specimens having slits whose inclination varied from 15° to 75°.

As seen Fig. 4, it can be stated that the peak strength and the elastic modulus inclease with increasing slit angle. It is obvious that the larger slit angle is, the smaller the projected section area of slit area in the loading direction. Therefore, the stress increases in proportion to the rotation of slit clockwise.

Furthermore, by consisting experimental

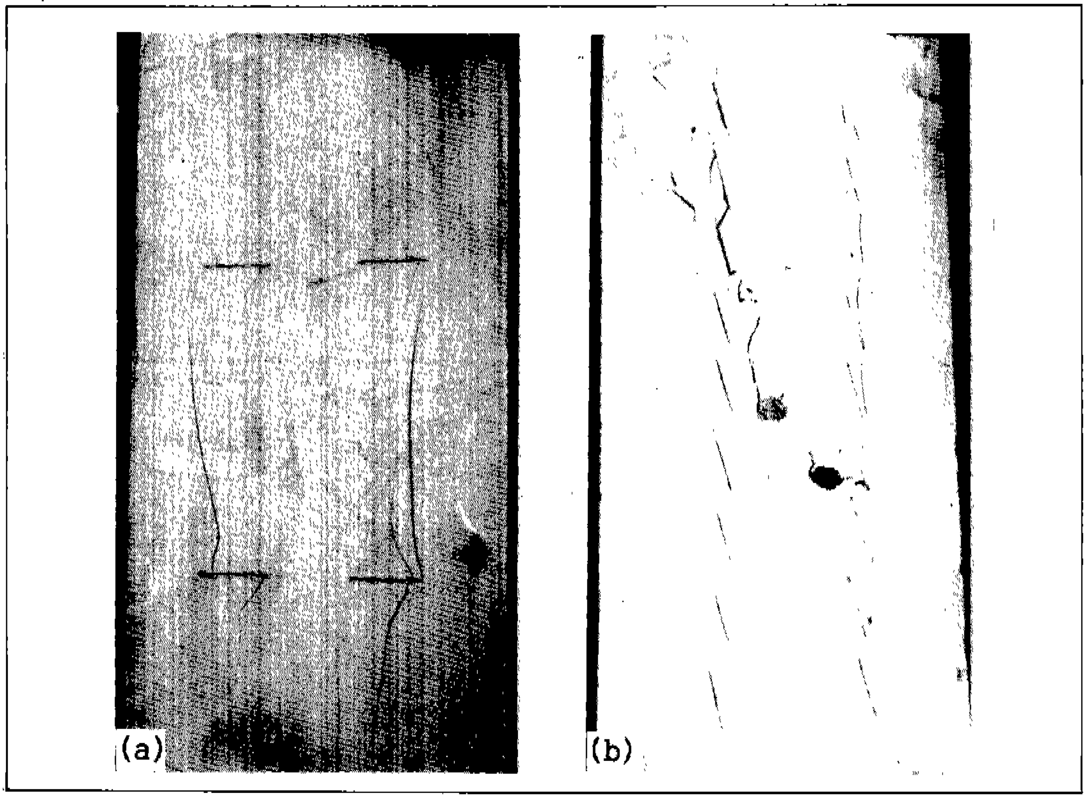

Fig.3 Cracked mortar specimen for experiments ; (a)θ=0°, (b) θ=75°.

data regarding the normalized peak strength and elastic modulus, it can be seen that the greater slit angle is, the greater the ratio of them is (Fig. 5). But the rate of these ratios decreases in proportion to increasing slit angle. As the slits are very thin, the influence of the thickness on them may be neglected (Aydan et al., 1992).

From the relation between the peak strength and slit angle, it can be stated that the peak strength monotonically increases as the slit angle increases (Fig. 6). This is different from the case of the normalized elastic modulus. It implies that the ratio may be different for elastic behavior from plastic behavior. Therefore, the peak strength is regarded as the strength of the remaining columns at the final stage of crack propagation. In the other words, at the peak state, it indicates that the larger the slit angle is, the wider the columns, which the load is supported are.

Crack Initiation and Propagation

We attempted to determine an index for the initial yielding point from the crack initiation during the testing of specimens. Since the point of initiation depends on the visibility of cracks, it was difficult to do so.

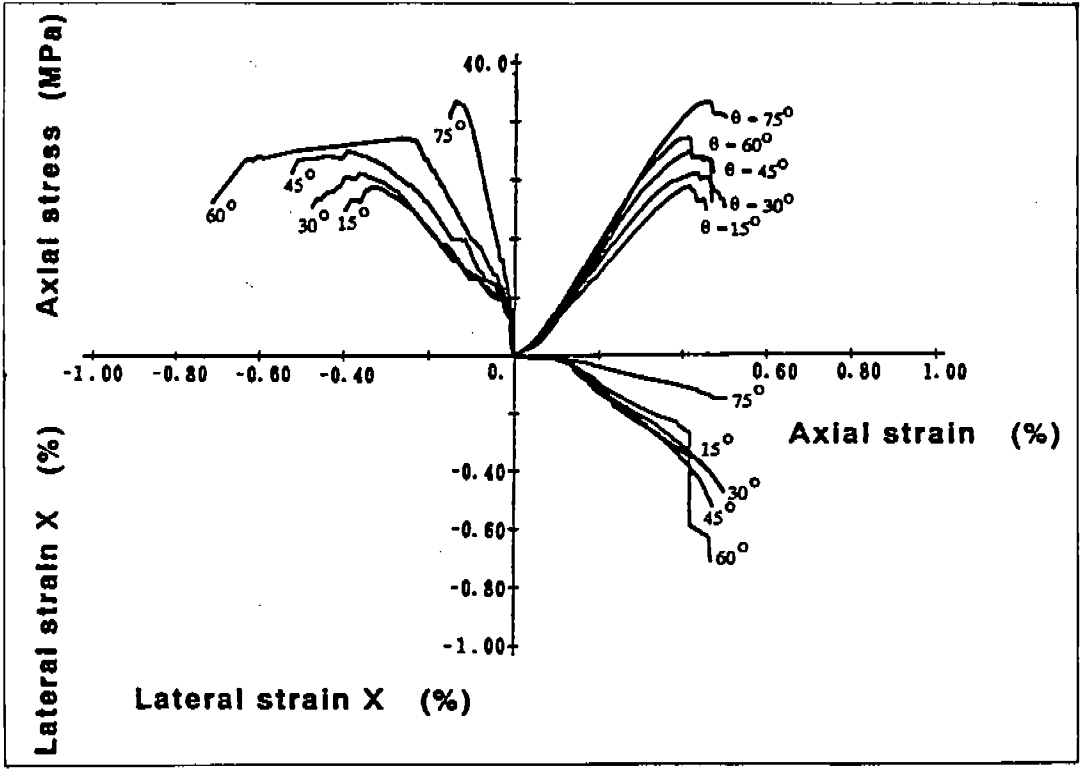

Fig.4 Axial stress, axial strain and lateral strain relation for each slit inclination.

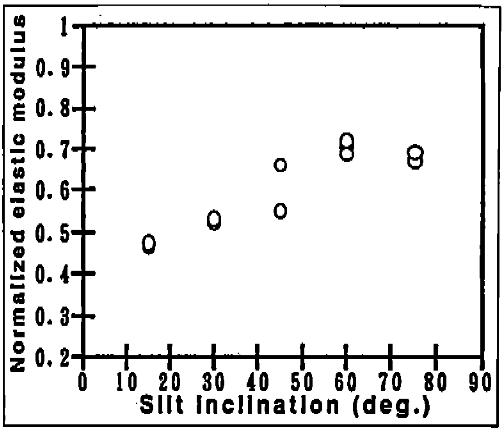

Fig.5 Relation between the normalized elastic modulus and slit inclination.

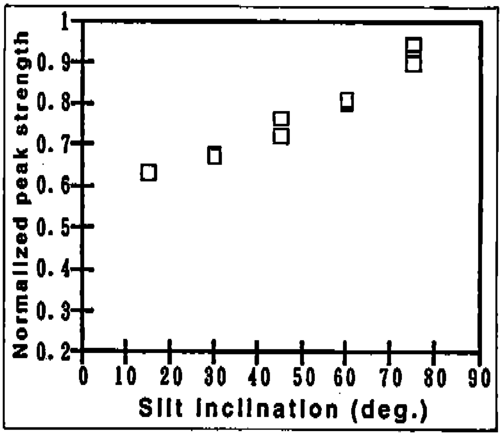

Fig.6 Relation between the normalized peak strength and slit inclination.

Therefore, we determined the initial yielding point from X−direction response of the axial stress and the lateral strain. If this index can be determined from the relation between the axial stress and the axial strain, it is an ideal index. As the marked variation can not be observed from the relation, we ultimately paid attention to the marked increase of lateral strain in X−direction occurred in tests. This marked variation can be seen in almost all tests. As a result we assumed this index as the point of crack initiation.

The propagation length was determined as a line length of the line connecting the point of crack initiation to the crack tip, and the propagation inclination was defined as the angle between slit and that line. The crack propagation is mainly observed for 0° slit angle. From the results of crack propagation, the onset points of cracks were observed not only at the both slit tips, but also at some locations between slip tips.

The latter may mean that the thickness of slit influences the crack initiation. The tension area exists on the upper and lower sides of the slit. For this reason, it is deemed that the crack propagates from the upper or lower sides.

NUMERICAL ANALYSIS OF TESTS

Theoretically, the initial yielding point must be associated with the crack initiation. Because of the assumed index to determine the crack initiation, it became obvious that observed crack initiation may or may not directly correspond to that determined from tests, and it is always not easy to see the initiation of cracks during tests. Therefore, we made a plane strain finite element to have a fine picture of the stress state around slits. Since the specimen had a periodic slit set, a unit cell having one slit was selected. Fig. 7 shows the finite element mesh of the unit cell and boundary conditions.

In general, the stress at crack tip must be calculated by using a special element in FEM or applying BEM (Washizu et al., 1983). In this study our purpose is to predict the stress state around the slit rather than that at a crack tip. In the analysis 4−nodded isoparametric elements were used and a fine meshing around the slit tips was adopted. In FEM analysis the slit angle was varied from 0° to 90° by an increment of 15°. We use the mechanical properties given in Table 1.

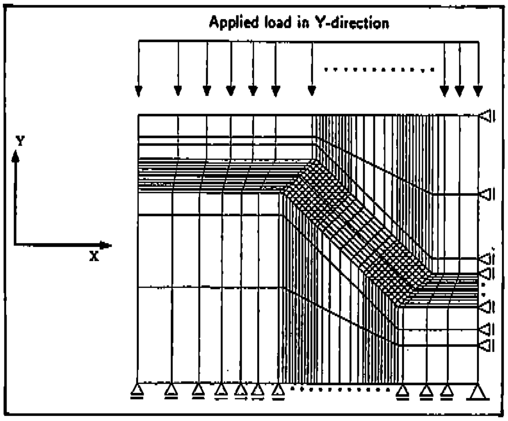

Fig.7 FEM mesh including one slit and boundary condition(θ=45°).

Table 1 Mechanical properties of mortar

Elastic modulus(E)	1.43×10^4	(MPa)
Poisson's ratio(ν)	0.09	
Internal friction angle(φ)	35.0	(deg.)
Cohesion(c)	9.57	(MPa)
Tensile strength(σ_t)	5.00	(MPa)

The applied tractions were 5 MPa and 10 MPa to calculate the yielding around the slit. At first, we determined the element which has the minimum safety factors for shear yielding (SFS) and tension yielding (SFT). The minimum applied load at shear yielding for each slit inclination was determined by using the Mohr−Coulomb criterion. We predicted yield stress by shearing failure by using maximum principal stress (σ_1) and minimum principal stress (σ_3) which were selected by using the minimum SFS and material parameters. And we also predicted the tensile yielding stress by using tension−cut concept. The relation between the applied load and the predicted initial shear and tensile yield stresses for each slit inclination is obtained as shown in Fig. 8.

As expected, the selected element which has the minimum safety factor was almost located in the vicinity of slit tips except for 0° inclination. From these relations, we obtained a relation between the slit angle and the applied load at the time of initial yielding for shear and tension. These relations and experimental data of initial yield stress are plotted in Fig.9.

As seen Fig. 9, the failure may occur by tension for almost all slit inclinations. For inclina-

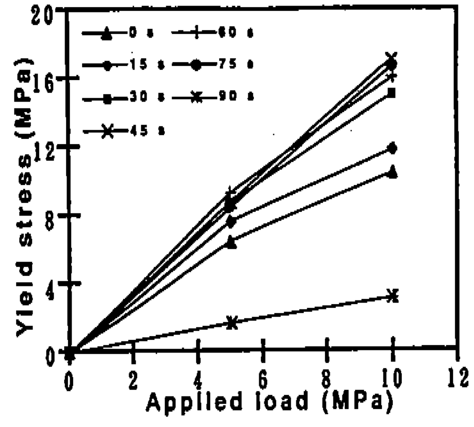

(a) SFS

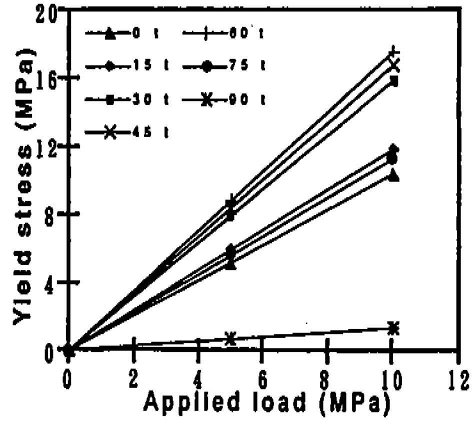

(b) SFT

Fig.8 Relation between the applied load and initial yielding stress ; (a) SFS, (b) SFT.

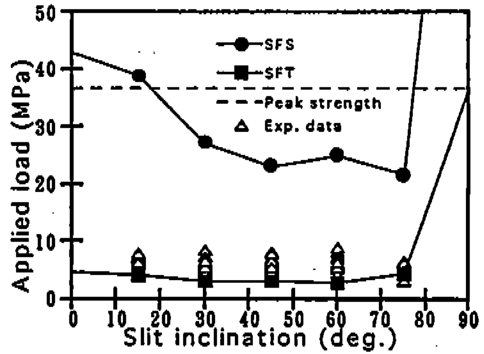

Fig.9 Relation between the applied load at initial yielding and slit inclination.

tion exceeding 75°, the applied load for the initial yielding becomes very large. This tendency was also supported by the observation on experiments. The relation between the applied stress and experimental data means that the initial yielding may occur mainly due to tensile stresses. Tensile stress distribution was calculated at crack tip by Homogenization theory (see Jeong, 1993). Local values of the tensile stress normalized to the loading stress in the vicinity of crack tip are shown in Fig. 10. As a result, the maximum value of the local tensile stress at crack tip is 21% of loading stress.

On the other hand, the yield stress by shearing failure (SFS) is obviously different from experimental data. This does not mean that there is no relation between the initial yielding and shear failure. We can see that applied load by SFS has lower values than the peak strength (36.6 MPa) for slit inclinations from 30° to 75°. This means that the secondary yielding or secondary crack propagation may occur due to shearing.

The principal stress directions at each Gaussian point of the elements were calculated. From these, the possible fracture angles for shear and tension modes were also calculated. The predicted orientations are compared with the experimental data and the predictions by the Sih's theoretical results (Sih, 1991) for the mixed fracture mode (Poisson's ratio=0.1). These results are plotted in Fig. 11.

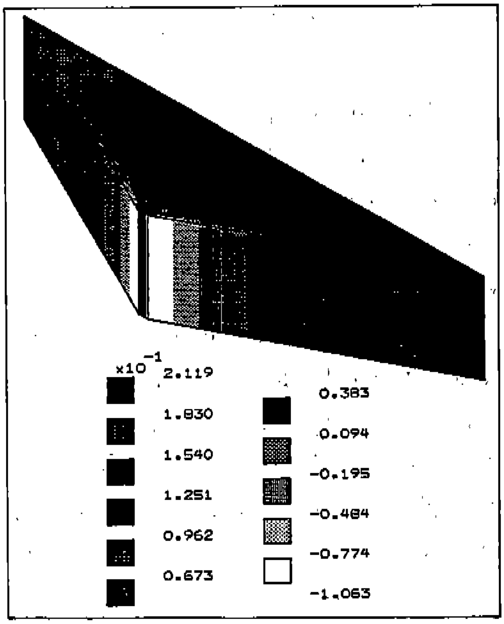

Fig.10 Stress concentration at crack tip.

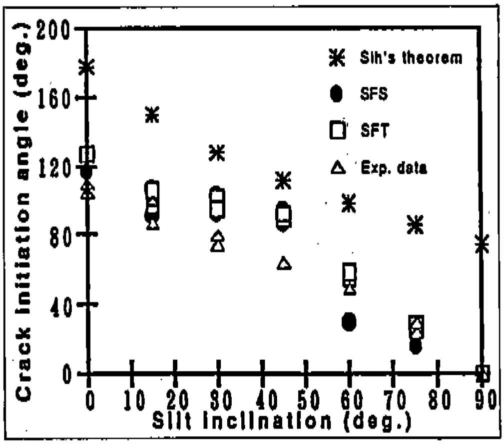

Fig.11 Relation between the slit angle and the angle of initial crack propagation.

As noted from Fig. 11, the finite element predictions almost coincide with the experimental data. Furthermore, the finite element predictions are much closer to the experimental data than those predicted by the Sih's theorem.

CONCLUSIONS

In this study, we investigated the mechanical effect of cracks on the behavior of rock with biotite contents. For this purpose, we tested specimens of mortar having one crack set which has a constant length and same direction. And orientation of this set was varied with respect to the loading axis. The experiments have analysed by FEM and Homogenization theory by modelling specimens and its geometry explicitly. Test results have shown that the crack set has a considerable effect on the macroscopic mechanical properties of a medium having distributed cracks.

A macroscopic continuum model based on the consideration of the mechanical effect of periodic cracks can fairly predict the averaged macroscopic mechanical properties (Aydan et al., 1992). However, these models are not sufficient to predict the initial yielding. When a specimen having many slits was tested under uniaxial compression, it is difficult monitor the crack propagation process. Nevertheless, it is possible to observe the crack initiation and the orientation and length of cracks in relation to the stress－strain response. The crack initiation and propagation may be predict by FEM and the stress concentration at the crack tip may be also calculated by Homogenization theory. The comparison of experimental data with prediction have shown that the analytical models are fairly sufficient to predict the effect of cracks on the mechanical response of rocks having cracks.

REFERENCES

Aydan, Ö., Seiki, T., Tokashiki, N., and Ito, F., 1992, Deformability and strength of discontinuous rock masses. Proc. Int. Symp. Fractured and Jointed Rock Mass. Lake Tahae. 2, pp.256－263.

Brace, W. F., and Walsh, J. B., 1962, Some direct measurements of the surface energy of quartz and orthoclase. Am. Mineral., 47, pp.1111－1122.

Gottschalk, R. R., Kronenberg, A. K., Russel, J. E., and Handin, J., 1990, Mechanical anisotropy of gneiss : Failure criterion and textural sources of directional behavior. J. Geophy. Res., 95, pp.21613－21634.

Jeong, G. C., Ichikawa, Y., and Kawamoto, T., 1993, Direct observation of microcracking and subsequent failure in quartz－feldspar rock (bisphere) under uniaxial compression. Int. Symp. on Assessment and Prevention of Failure Phenomenon in Rock Engineering. Istanbul, A.A.Balkema, pp.335－341.

Jeong, G. C., and Ichikawa, Y., 1994, An experimental study on damage propagation of intact granite. J. Society of Materials Sciences, Japan, Vol.43, No.486, pp.317－323.

Jeong, G. C., and Ichikawa, Y., 1993, An analysis of stress concentration in major minerals of granite by homogenization method. Proceeding of the 7th Japan Computational Mechanics Symp., pp.229－236.

Seiki, T., Ichikawa, Y., Aydan, Ö., and Ito, F., 1993, Mechanical behavior and failure of rock masses having distributed sets of cracks of finite length. Int. Symp. on Assessment and Prevention of Failure Phenomenon in Rock Engineering. Istanbul, A.A.Balkema, pp.181−186.

Shea, W. T., and Kronenberg, A. K., 1993, Strength and anisotropy of foliated rocks with varied mica contents. J. Struct. Geol., 15, pp.1097−1121.

Sih, G. C., 1991, Mechanics of fracture initiation and propagation. Dordrecht, Kluwer Academic Publishers, 540p.

Wong, T. F., and Biegal, R., 1985, Effects of pressure on the micromechanics of faulting in San Marcos gabbro. J. Struct. Geol., 7, pp.737−747.

Washizu, H., Miyamoto, H., Yamada, Y., Yamamoto, Y., and Kawai, T., 1983, FEM handbook II Applied edition, Baifuukan, Tokyo, (in Japanese).

김영기 :
경북대학교 지질학과
대구직할시 북구 산격동
702−701
TEL : (053)950−5357
FAX : (053)957−0431
정교철, 김원영 :
한국자원연구소
대전직할시 유성구 가정동 30번지
305−350
TEL : (042)868−3050
FAX : (042)861−9720
清木隆文,市川康明 :
Dept. of Geotechnical and
Environmental Engineering
Nagoya University
Furo−cho, Chikusa−ku
Nagoya, 464−01 Japan
TEL : 001−81−52−789−3830
FAX : 001−81−52−789−3837